Repeated Load Model for Subgrade Soils: Model Development

LUTFI RAAD AND BASSAM A. ZEID

A load deformation model for subgrade soils is developed, where total cumulative axial strains are correlated with applied stresses and number of load repetitions. The model is based on the results of repeated load tests for a compacted silty clay. The concept of a constant failure strain independent of load history is presented and used in the proposed model. Results of static triaxial tests, slow cyclic tests, and repeated load tests are used to verify that the failure strain for given compaction conditions and confining pressure is essentially independent of stress history. Good agreement is obtained between predicted strains and experimental values from repeated load tests. Model predictions are within ±10 percent of experimental results.

Modern techniques for pavement design and analysis utilize limiting response criteria to control cracking and rutting in pavement structures. The behavior of the subgrade, in this case, could be of major significance to the overall performance of the pavement. The resilient behavior of subgrade soils has been defined in terms of repeated stresses and recoverable or elastic strains. Those relations have been incorporated into multilayer analyses for the purpose of predicting the resilient response of pavements under repeated traffic loads (*1–3*). Limiting values in the critical response parameters are proposed by many rational design methods as a means of achieving satisfactory pavement performance. In the case of subgrade soils, such criteria are presented in terms of strains, normal stresses, and deviator stresses on top of the subgrade layer. Those criteria have been determined in two different ways: first, through the use of structural models to analyze pavements of known performance (*4–7*) and, second, through laboratory testing of specimens under repeated stress applications (*8–10*). Other permanent deformation models, such as those proposed by Barksdale (*11*), Knutson et al. (*12*), and Monismith et al. (*13*), could be used to estimate the magnitude of subgrade strains for a different number of load applications. Some limitations of those criteria and permanent deformation models are summarized:

1. Subgrade normal strain criteria are derived through back-calculation procedures by using multilayer elastic analysis of pavements with known performance and, therefore, ignore the stress-dependent behavior of the pavement materials. Moreover, those criteria are suitable for similar pavement conditions and are not applicable, in general, to conditions of different pavement loading, materials, geometry, and environment.

L. Raad, Institute of Northern Engineering, University of Alaska, Fairbanks, Alaska 99775. B. A. Zeid, Dar Al-Handassah (Shair and Partners), Beirut, Lebanon.

2. Subgrade normal stress or strain criteria derived from laboratory tests do not explicitly account for the influence of changes in subgrade soil type, density, moisture content, and stress state on the accumulation of plastic strains under field-loading conditions. Those criteria, expressed in terms of limiting stresses or strains, are based on applicable permanent strain levels in laboratory specimens and do not provide the mechanism for predicting permanent strains in the subgrade.
3. Although available permanent strain models can be used to estimate the permanent deformations in the subgrade, the models do not provide an assessment of subgrade failure in terms of increased rate of plastic strain accumulation. Those failure conditions need to be incorporated in advanced analyses of pavements for the purpose of improving pavement response and performance predictions (*2,14*).

The development of improved stress-strain models should describe the load-deformation and strength behavior of compacted fine-grained subgrade soils under repeated loads. Those would be considered in lieu of reported findings that suggest that failure strain is generally independent of loading rate or type but depends mainly on the initial conditions of the specimen (i.e., initial stress state, density, and moisture content). Experimental work conducted by Vaid and Campanella (*15*) on undisturbed Haney clay indicates that for given testing conditions, irrespective of the creep stress level, rupture occurs approximately at the same magnitude of axial strain and that this is equal to the failure strain in conventional constant strain rate undrained shear testing. Similar observations were reported by Mitchell (*16*) on the failure strain of different types of undisturbed clays under creep loading. More recently, data provided by Ansal and Erken (*17*) on the behavior of one-dimensionally consolidated Kaolinite clay under cyclic simple shear testing show that the cyclic shear strain amplitude corresponding to the cyclic yield strength remains essentially constant for different numbers of stress cycles. Zeid (*18*) investigated the behavior of a compacted silty clay under different forms of loading that included static tests, creep tests, and repeated load tests. Results illustrate that the failure strain for a given confining pressure, dry density, and compaction moisture content remains essentially constant, independent of the type of the test performed.

Results of static triaxial tests, slow cyclic load tests, and repeated load tests for a compacted silty clay are presented here to illustrate the concept of a constant failure strain, independent of stress history. This concept is used in the development of a load-deformation model for subgrade soils, where total strains are correlated with repeated stresses and number of load repetitions. Strain predictions, using the proposed model, are compared with experimental results from repeated load tests.

EXPERIMENTAL WORK

Testing Procedure

Strain-controlled static triaxial tests, stress-controlled slow cyclic load tests, and stress-controlled repeated (transient) load tests were conducted on a compacted silty clay in the undrained mode. The identification properties of the soil used are summarized in Table 1. The soil was compacted in a California bearing ratio (CBR) mold according to the modified AASHTO method (ASTM D1557-66T). Specimens were then extruded by using thin wall brass tube samplers and trimmed to 1.5-in diameter and 3.0-in height. Each specimen was placed between a cap and a base, encased in two rubber membranes, and cured in a water bath until ready for testing.

Two series of static triaxial tests were performed on specimens, which were cured for 24 hr and had dry densities and compaction moisture contents covering the range defined by modified AASHTO compaction. In the first series, the specimens were subjected to a confining pressure of 14.5 psi and then were loaded to failure at strain rates equal to 0.084 percent/min, 0.50 percent/min, and 1.96 percent/min. In the second series, the specimens were tested at a strain rate of 0.50 percent/min at confining pressures of zero, 14.5 psi, 29 psi, and 58 psi.

Cyclic load tests and repeated load tests were conducted on specimens cured for 2 weeks. Those specimens had a dry density of 129.5 lb/ft^3 and compaction moisture content corresponding to optimum ± 1.5 percent. The maximum dry density and optimum moisture content given by modified AASHTO compaction were 131.5 lb/ft^3 and 8.5 percent. The allowable range of variation for dry density and compaction moisture content for the tested specimens was ± 0.6 lb/ft^3 and ± 0.25 percent, respectively.

A confining pressure of 14.5 psi was used for the cyclic load tests. The specimens were then subjected to cyclic deviator stresses that had essentially a rectangular shape and a duration of 0.50 min at a frequency of 1 cpm. The specimen was immediately loaded to failure at a constant rate of strain following the applications of a specific number of load cycles. The strain rates used were 0.084 percent/min and 1.96 percent/min. The cyclic stresses corresponded to 50 percent and 80 percent of the strength associated with the applied strain rate at the end of the cyclic period. The number of stress cycles of each stress level applied were 10, 50, 100, and 150.

TABLE 1 IDENTIFICATION PROPERTIES OF SILTY CLAY USED

Parameter	Value
Liquid limit	28
Plasticity index	11
Specific gravity	2.708
Percent finer than 0.074 mm	80
Clay fraction (percent less than 0.002 mm)	18
Unified Classification	CL
AASHTO Classification	A-6(7)

In the repeated load tests, specimens were tested in the unconfined state and at a confining pressure equal to 14.5 psi. Pneumatically controlled deviator stress pulses having an approximate triangular shape and average duration of 0.2 sec were applied at a frequency of 40 cpm. Stress levels of 0.70, 0.80, 0.90, and 0.95 were used. The stress level is defined in this case as the ratio of repeated deviator stress to the strength obtained from a standard triaxial test at a strain rate of 0.5 percent per minute. For a given repeated stress level, the axial strains were monitored with number of load repetitions. A summary of testing conditions and strength properties of the silty clay used in this study is presented in Tables 2 and 3, respectively.

Results

Results of triaxial tests presented in Figures 1 and 2 indicate that the failure strain ϵ_f, defined as the axial strain at peak

TABLE 2 TESTING CONDITIONS FOR THE SILTY COMPACTED CLAY

Test Type	Confining Pressure (psi)	Stress Level	Strain Rate (% per min)	Frequency and Shape	Duration (sec)	Number of Cycles
Strain Controlled Static Triaxial Test						
- Series 1	14.5	-	0.084,0.50, 1.96	-	-	-
- Series 2	0,14.5,29,58	-	0.50	-	-	-
Stress Controlled Cyclic Test	14.5	0.50, 0.80	0.084,1.96,	1 cpm (rectangular)	30	10,50, 100, 150
Repeated Load Test	0, 14.5	0.70,0.80, 0.90,0.95	-	40 cpm (triangular)	0.20	to failure or 10^4

NOTES

- In the strain-controlled static triaxial tests, the dry density and compaction moisture content of specimens covered the range defined by modified AASHTO compaction. Specimens were cured for 24 hours prior to testing.
- In the cyclic and repeated load tests, specimens were compacted to a dry density of 129.5 lb/cu ft and moisture content of 7.0 percent and 10 percent. Specimens were cured for two weeks prior to testing.
- The maximum dry density and optimum moisture content associated with modified AASHTO compaction were 131.5 lb/cu ft and 8.5 percent respectively.

TABLE 3 SHEAR STRENGTH CHARACTERISTICS OF THE SILTY CLAY

Compaction Properties	Cohesion C (psi)	Angle of Friction ϕ(degrees)	Undrained compressive strength σ_{df} (psi)	
			$\sigma_3 = 0$	$\sigma_3 = 14.5$ psi
γ_d = 129.5 lb/cu ft, m = 7 %	39.0	32	140	173
γ_d = 129.5 lb/cu ft, m = 10 %	23.0	32	83	117

NOTES

- Shear strength properties were determined using strain-controlled undrained triaxial tests with rate of applied strain equal to 0.50 percent per minute.
- σ_{df} is equal to the difference of major principal stress σ_1 and minor principal stress σ_3 at failure.

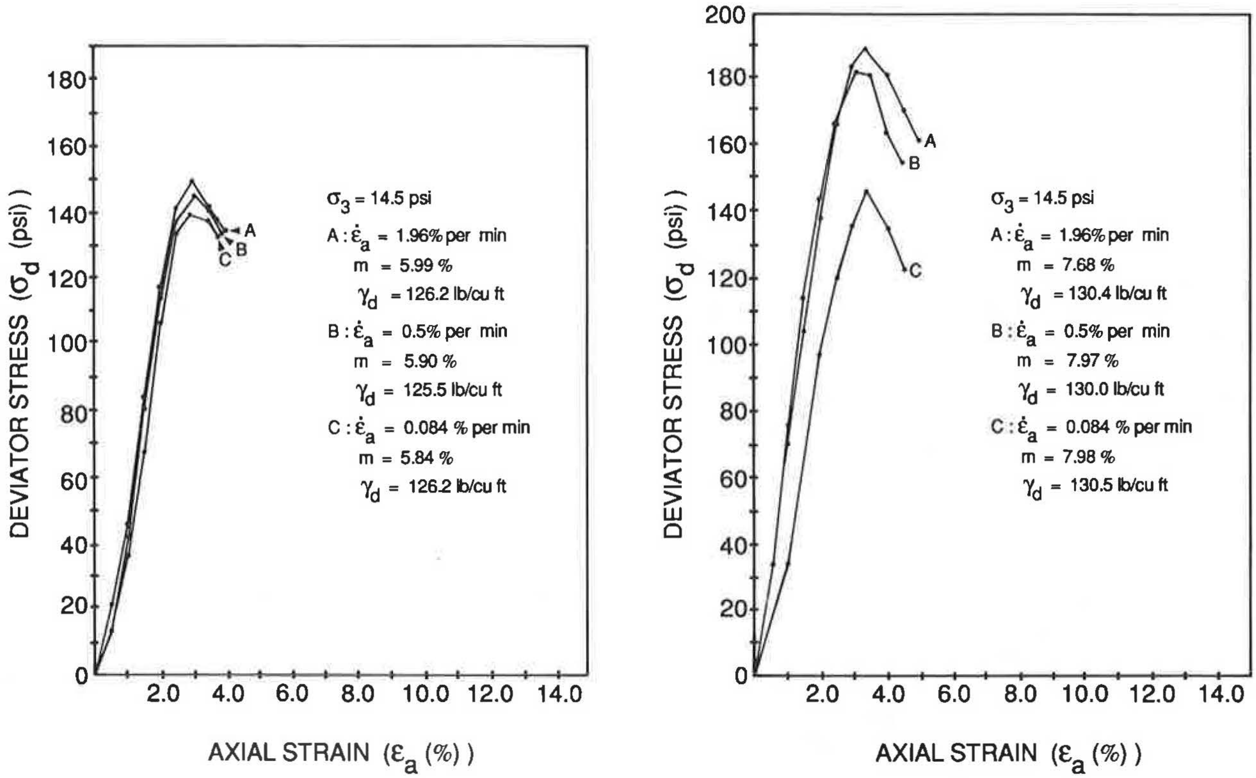

FIGURE 1 Stress-strain behavior for specimens compacted dry of optimum.

deviator stress, seems to be relatively independent of applied strain rate $d\epsilon_a/dt$ for a given confining pressure σ_3, dry density γ_d, and compaction moisture content m. Although the influence of strain rate on the strength can be significant, the variation of the strain at failure remains small. For example, the strength of specimens with average dry density of 130 lb/ft^3 and compaction moisture content of 7.88 percent exhibits a strength increase from 145 psi when subjected to a strain rate of 0.084 percent/min to 188 psi when the strain rate is 1.96 percent/min. The failure strain, however, remains in the range of 3.0 percent to 3.4 percent (Figure 1). The influence of confining pressure, compaction moisture content, and dry density on the failure strain is shown in Figure 3. An increase in confining pressure and compaction moisture content will result in higher failure strain values.

Similar observations are made in the case of the slow cyclic load tests, where cyclic deviator stress applications seem to have little effect on the failure strains as shown in Figures 4–7. The strength increases as the number of stress applications increases up to 50 cycles and then decreases with further increase in the number of cycles. The increase in strength is more significant for dry of optimum compaction conditions and lower cyclic stresses. Although the strength is influenced by cyclic stress history, the strain at failure remains virtually unaffected. In this case, the failure strain varies in the range of 2.8 percent to 3.2 percent for specimens compacted dry of optimum and 8.8 percent to 9.2 percent for specimens compacted wet of optimum.

Results of repeated load tests presented in Figures 8–11 illustrate the variation of total accumulated axial strain ϵ_a, defined as the sum of resilient strain and permanent strain, with the number of repetitions N of a given stress level q_r. The variation of the rate of accumulation of axial strain $d\epsilon_a/dN$ with the number of repetitions is also shown. The results indicate the existence of a "threshold stress level" below which the accumulation of axial strain will eventually cease and lead to a stable response and above which progressive accumulation of axial strains occurs and causes unstable response and ultimately failure. The "threshold stress level" for the repeated load tests performed lies between 0.80 and 0.90. Similar findings for a "threshold stress level" have been reported by other investigators (*19,20*). For repeated stresses larger than the "threshold value," the rate of axial strain $d\epsilon_a/dN$ decreases initially to a minimum value with the number of repetitions, after which it starts to increase. This flexure indicates a condition of incipient failure. This condition is conceived as a possible definition of failure under repeated loading, and the corresponding strains will be defined as failure strains. For example, failure strain values, obtained for a confining pressure of 14.5 psi, lie between 2.8 percent and 3.0 percent for specimens compacted dry of optimum and between 8.9 percent and 9.2 percent for specimens compacted wet of optimum. This agrees well with the failure strains obtained from cyclic load tests reported previously.

A summary of failure strain values for all the testing and compaction conditions used in this study is presented in Table

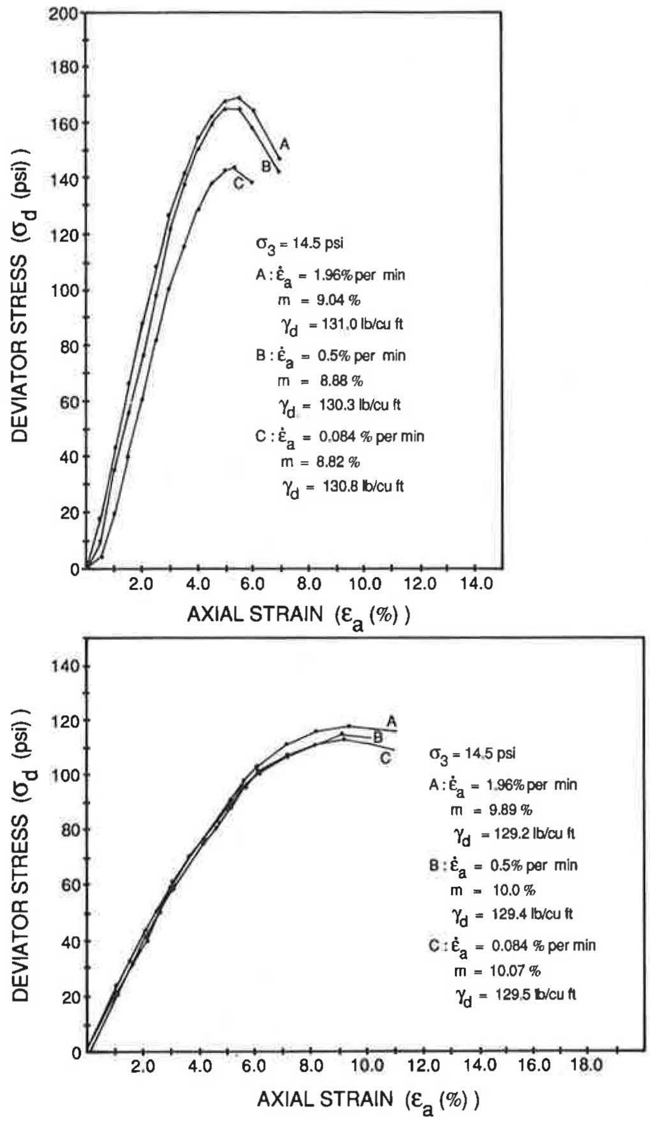

FIGURE 2 Stress-strain behavior for specimens compacted wet of optimum.

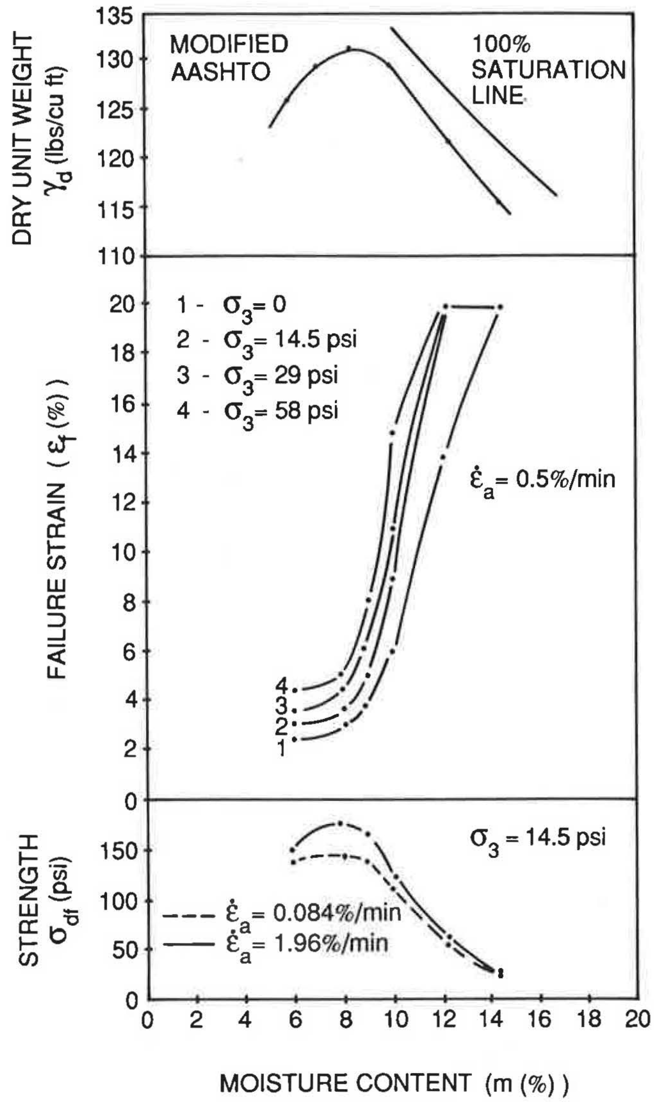

FIGURE 3 Variation of failure strain and strength for different compaction conditions.

4. Results indicate that for a given confining pressure, dry density, and compaction moisture content the failure strain is relatively independent of loading history and could, therefore, be determined from standard triaxial tests.

PROPOSED REPEATED LOAD MODEL

The behavior of the compacted silty clay in terms of axial strain ϵ_a, repeated load stress level q_r, and number of load repetitions N depends to a great extent on the magnitude of the applied stress level relative to the "threshold stress level" q_{rl}.

This behavior is schematically illustrated in Figure 12 for repeated stress level values less than q_{rl}. In this case, the variation of axial strain with the logarithm of number of repetitions can be represented by a transient state for N less than N_0, where the rate of axial strain decreases, and can be followed by a steady state where the rate of axial strain is relatively constant for N between N_0 and N_s and a stable state for N greater than N_s where no further accumulation of axial strain occurs with additional load repetitions. Repeated load test data on the compacted silty clay used in this study indicate that for q_r less than q_{rl} values of N_0 are generally less than 10, whereas N_s is less than 10^4. The range of practical interest for the variation of axial strain with number of load repetitions lies in the steady state region corresponding to N between N_0 and N_s. In this range, the experimental data seem to fit the following relation:

$$q_r = \frac{\epsilon_a}{a_L + s_L \log N} \tag{1}$$

where a_L and s_L are material parameters that can be determined from a plot of ϵ_a/q_r versus log N as shown in Figure 12.

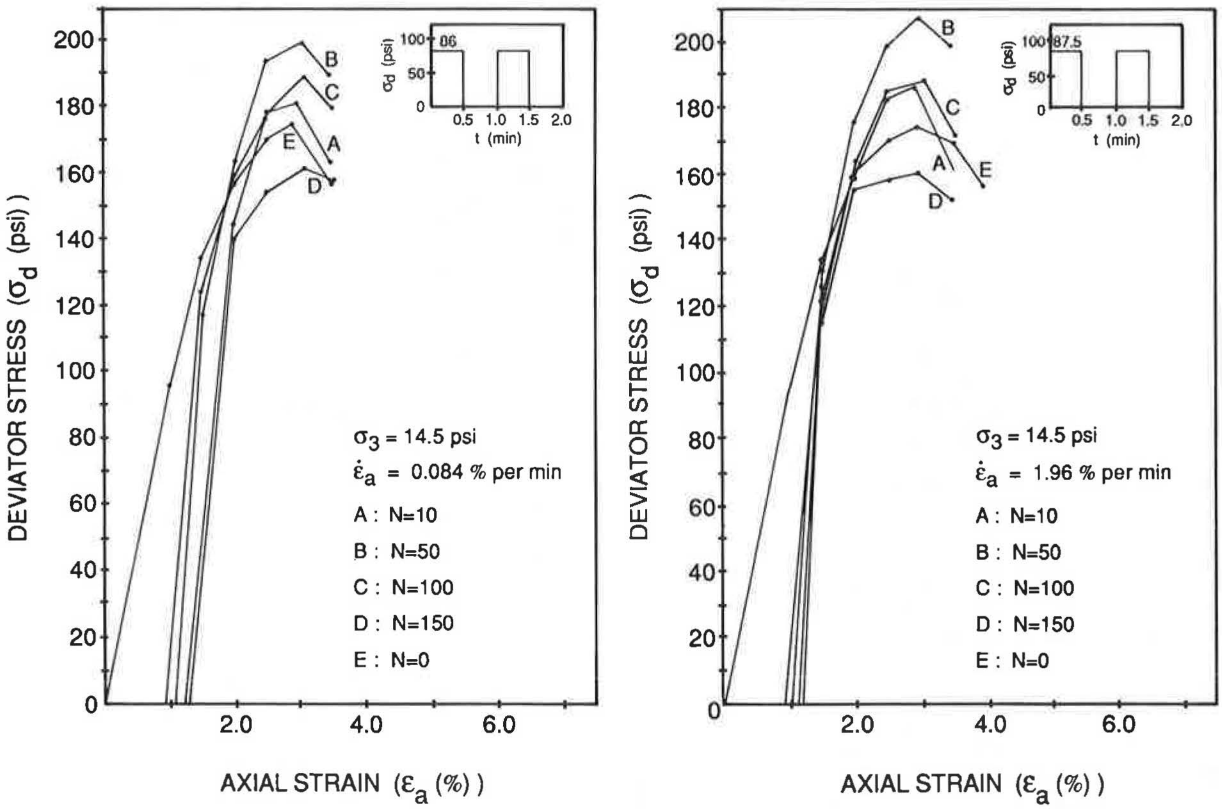

FIGURE 4 Load deformation behavior under 50 percent cyclic stress level (γ_d = 129.5 lb/ft^3, m = 7 percent).

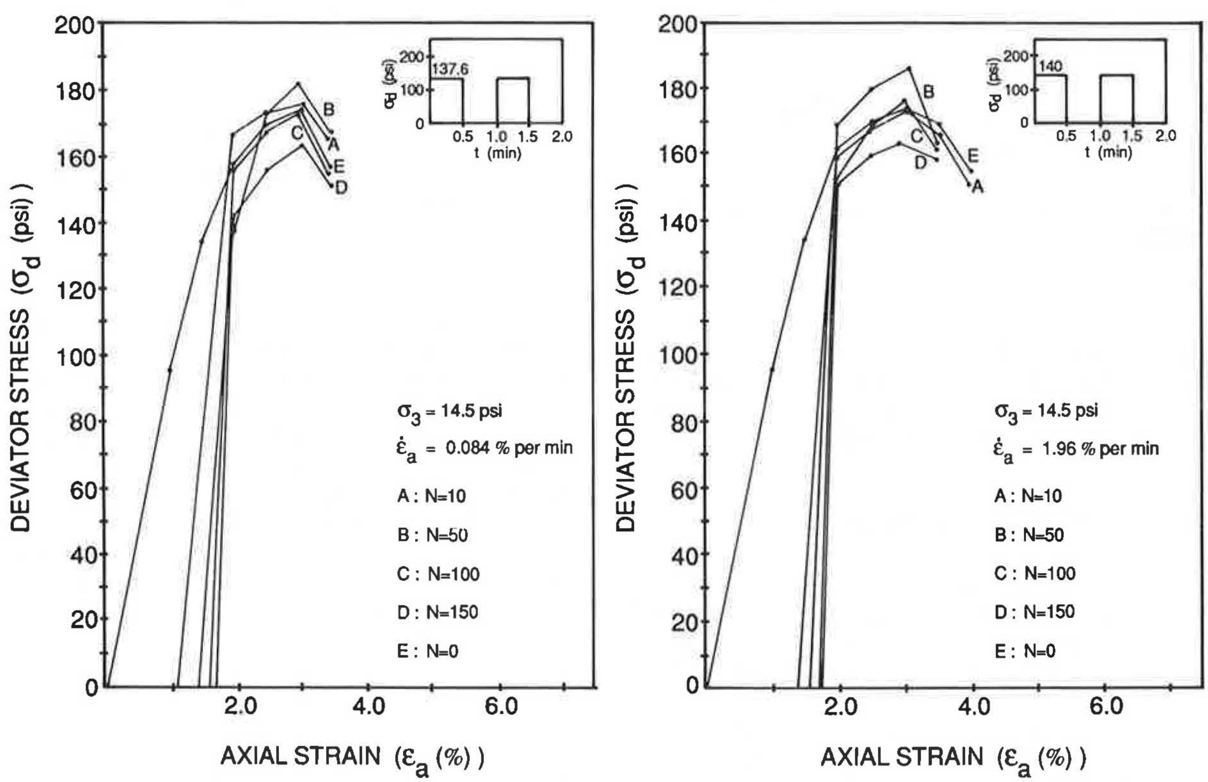

FIGURE 5 Load deformation behavior under 80 percent cyclic stress level (γ_d = 129.5 lb/ft^3, m = 7 percent).

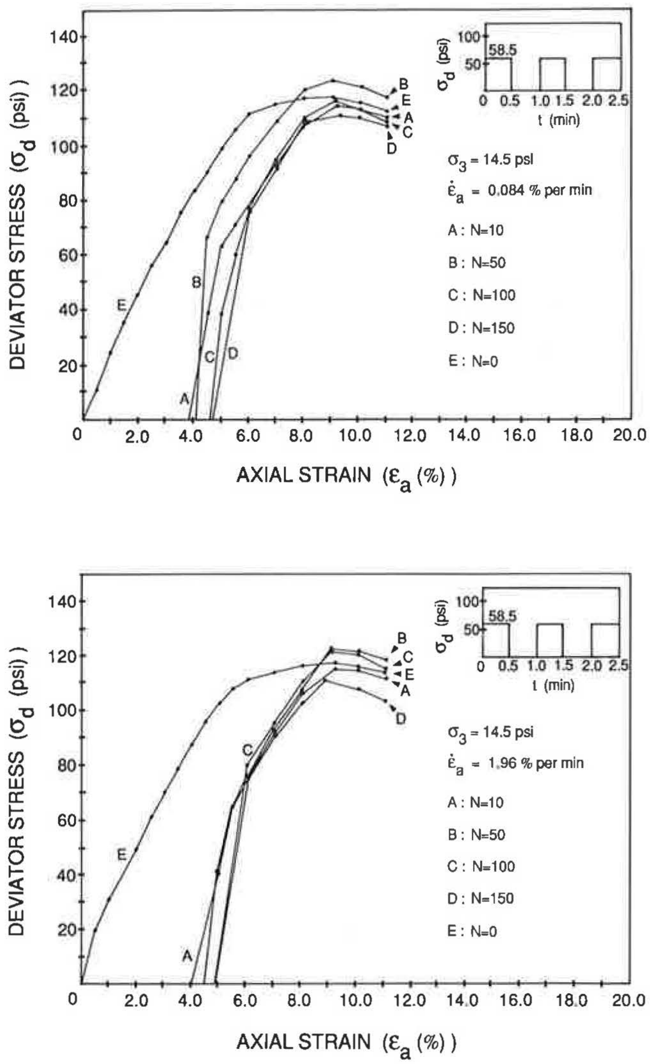

FIGURE 6 Load deformation behavior under 50 percent cyclic stress level (γ_d = 129.5 lb/ft^3, m = 10 percent).

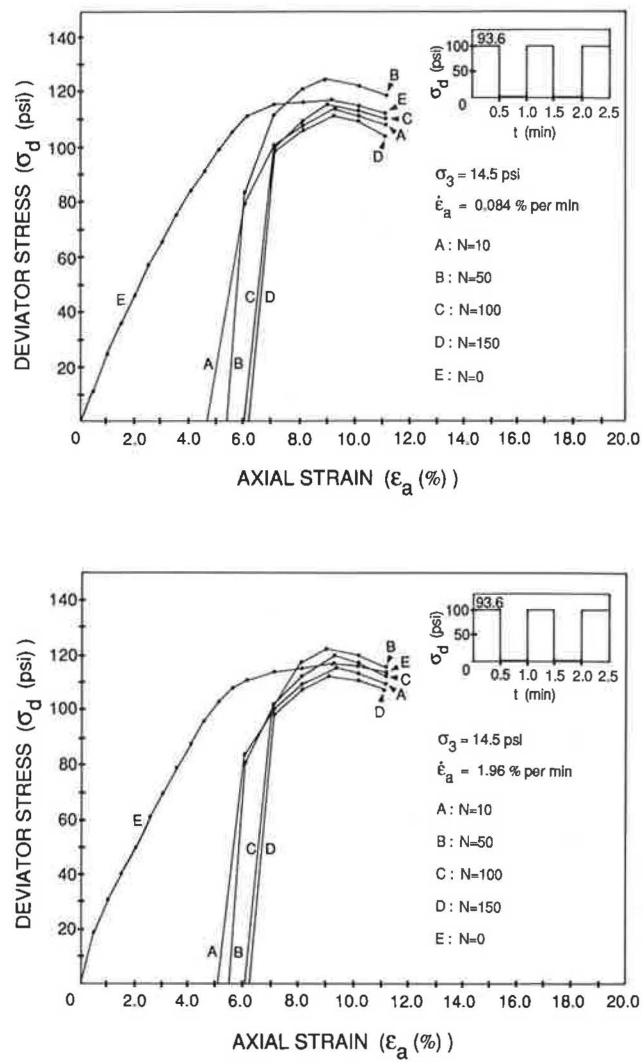

FIGURE 7 Load deformation behavior under 80 percent cyclic stress level (γ_d = 129.5 lb/ft^3, m = 10 percent).

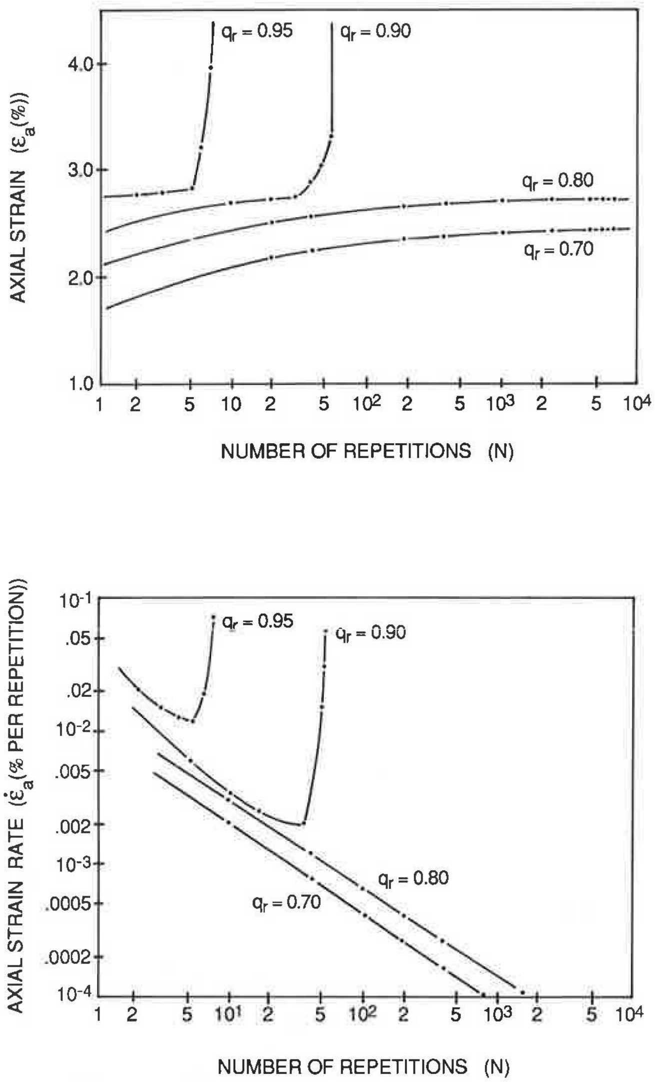

FIGURE 8 Variation of axial strain and axial strain rate with number of stress repetitions (σ_3 = 0, γ_d = 129.5 lb/cu^3, m = 7 percent).

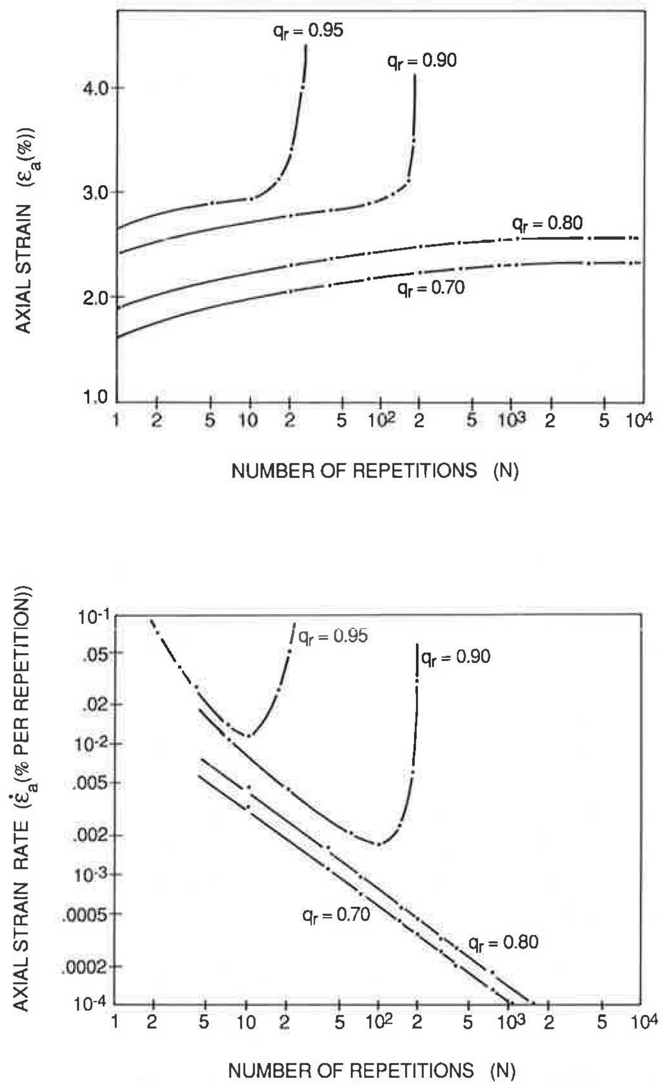

FIGURE 9 Variation of axial strain and axial strain rate with number of stress repetitions (σ_3 = 14.5 psi, δ_d = 129.5 lb/ft^3, m = 7 percent).

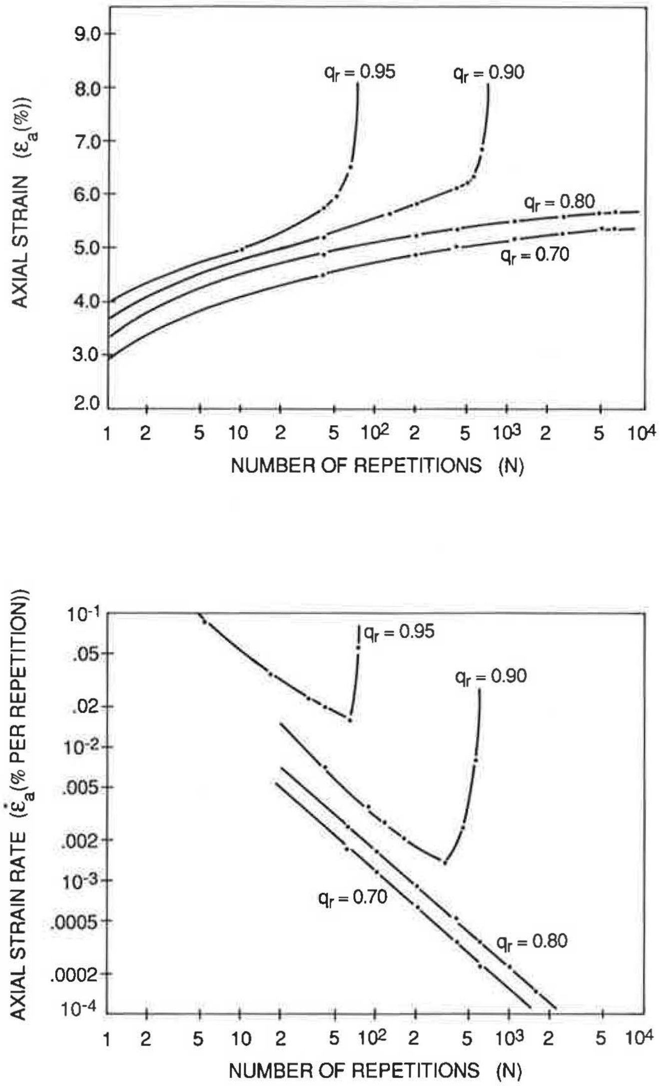

FIGURE 10 Variation of axial strain and axial strain rate with number of stress repetitions (σ_3 = 0, γ_d = 129.5 lb/ft^3, *m* = 10 percent).

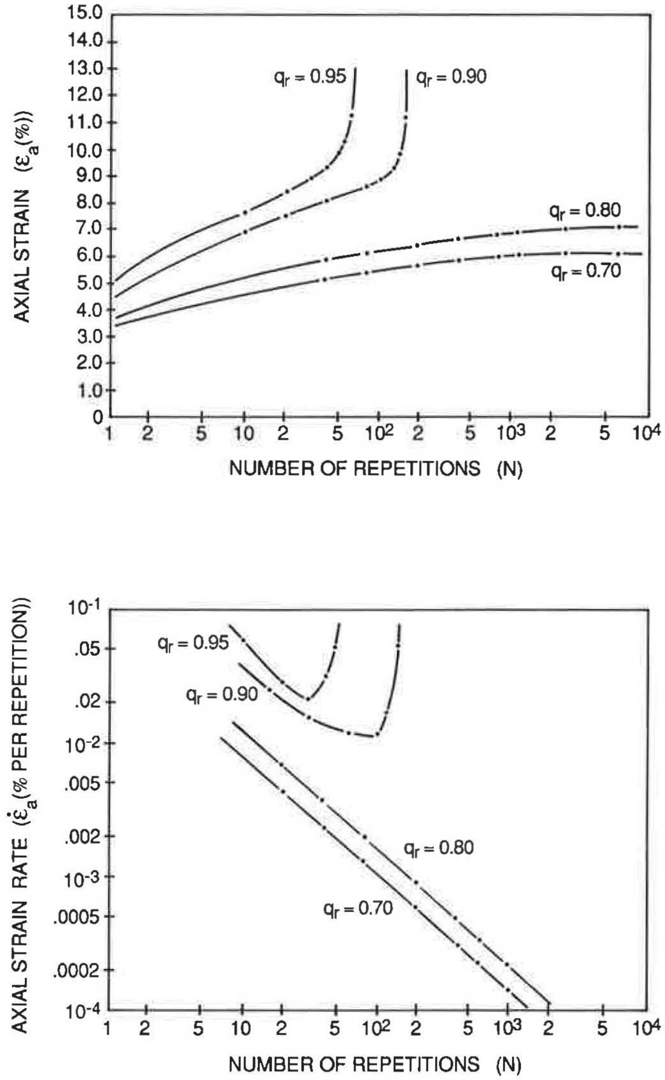

FIGURE 11 Variation of axial strain and axial strain rate with number of stress repetitions (σ_3 = 14.5 psi, γ_d = 129.5 lb/ft^3, *m* = 10 percent).

TABLE 4 VARIATION OF FAILURE STRAIN DETERMINED FROM TRIAXIAL, CYCLIC, AND REPEATED LOAD TESTS

Compaction Properties	Failure Strain, ϵ_f(%)	
	σ_3 = 0	σ_3 = 14.5 psi
γ_d = 129.5 lb/cu ft m = 7 %	2.70 - 2.90	2.80 - 3.20
γ_d = 129.5 lb/cu ft m = 10 %	5.90 - 6.20	8.80 - 9.40

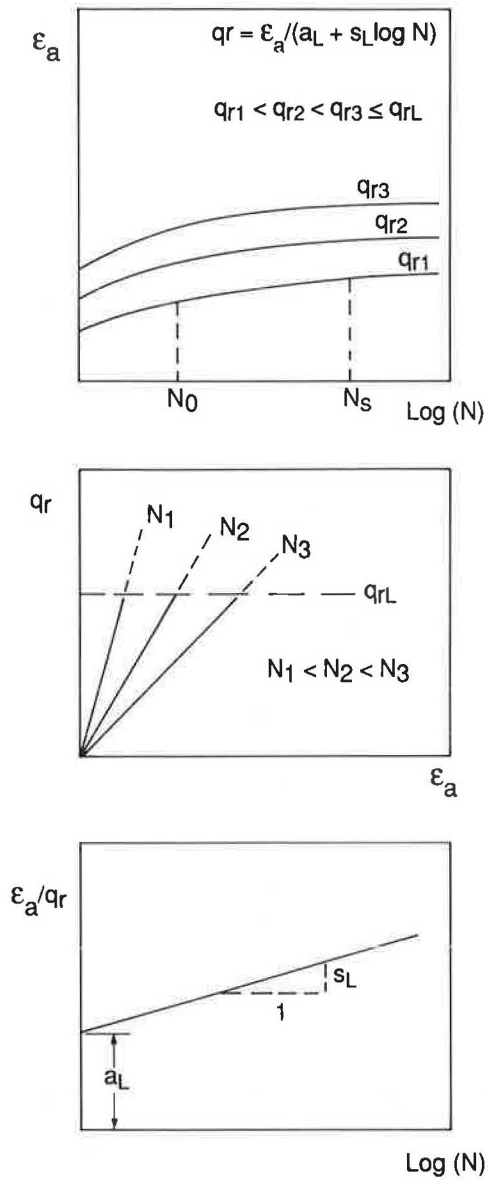

FIGURE 12 Schematic illustration of repeated load model for low stresses.

Repeated applications of stress level with a magnitude exceeding the "threshold value" lead initially to a transient variation of axial strain for N less than N_0, followed for larger N values by a steady state and then a tertiary state where the rate of axial strain will increase, leading eventually to failure when N reaches N_f. Values of N_0 were estimated to be generally less than 5. In the range where N is between N_0 and N_f, the repeated load data for axial strain, repeated stress level, and number of repetitions can be represented by the following relation:

$$q_r = \frac{\epsilon_a}{a_h + b_h \epsilon_a} \tag{2}$$

where

$$b_h = B_h + S_h \log N \tag{3}$$

and a_h, B_h, and S_h are material parameters.

Equation 2 indicates that the variation of q_r and ϵ_a for a given N is hyperbolic. For a given N, a_h and b_h can be determined from a plot of ϵ_a/q_r versus ϵ_a, as is indicated in Figure 13. Repeated load test data for the compacted silty clay were analyzed to determine material parameters in Equations 2 and 3. In this case, the variation of a_h for different values of N was found relatively insignificant, and the average a_h for

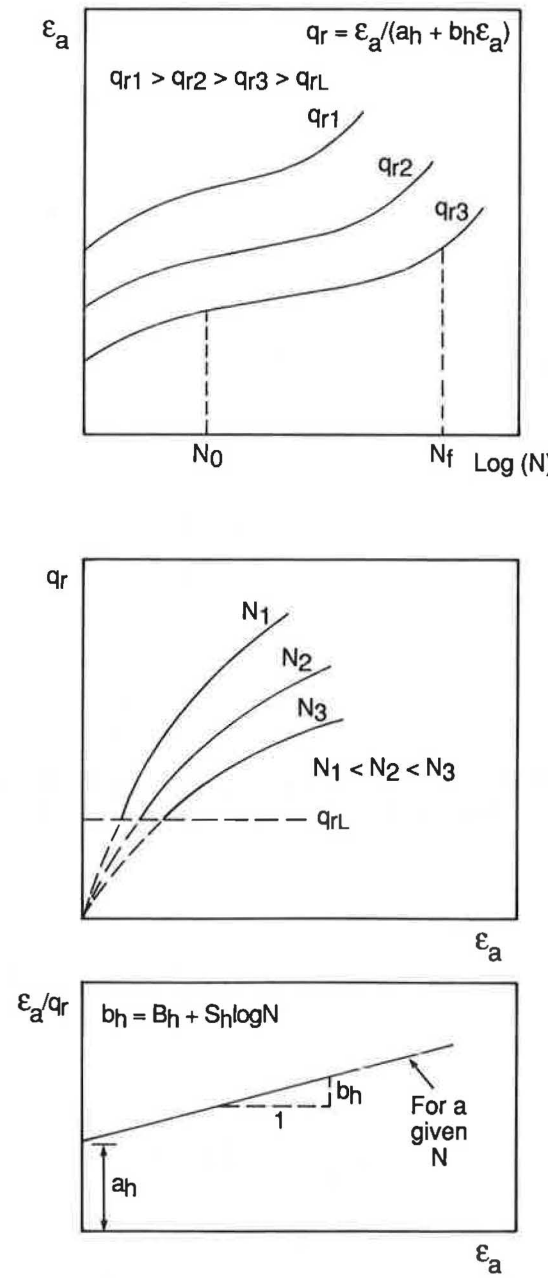

FIGURE 13 Schematic illustration of repeated load model for high stresses.

at least three selected values of N covering the range between N_0 and N_f was determined. The corresponding values of b_h were then used to find B_h and S_h in Equation 3.

The axial strain ϵ_a in Equations 1 and 2 is expressed in percent, and the corresponding material parameters are summarized in Table 5 for all testing conditions. Predictions using the proposed model are compared with experimental results in Figures 14 and 15. Model predictions of axial strains are within ± 10 percent of experimental values.

SUMMARY AND CONCLUSIONS

A load-deformation model for subgrade soils is developed, where total cumulative axial strains are correlated with applied stresses and number of load repetitions and is based on the results of repeated load tests conducted on a compacted silty clay. The concept of a constant failure strain independent of load history was used in the proposed model. Results of static triaxial tests, slow cyclic tests, and repeated load tests for the compacted silty clay were used to verify that the strain at failure for given compaction conditions and confining pressure is essentially independent of stress history. Good agreement was obtained between predicted strain values by using the proposed model and experimental values from repeated load tests. Model predictions were within ± 10 percent of experimental results.

ACKNOWLEDGMENTS

The experimental investigation presented in this paper was conducted at the American University of Beirut. Most of the analyses were performed at the University of Alaska, Fairbanks. The help provided by the Civil Engineering Department at both universities is greatly appreciated.

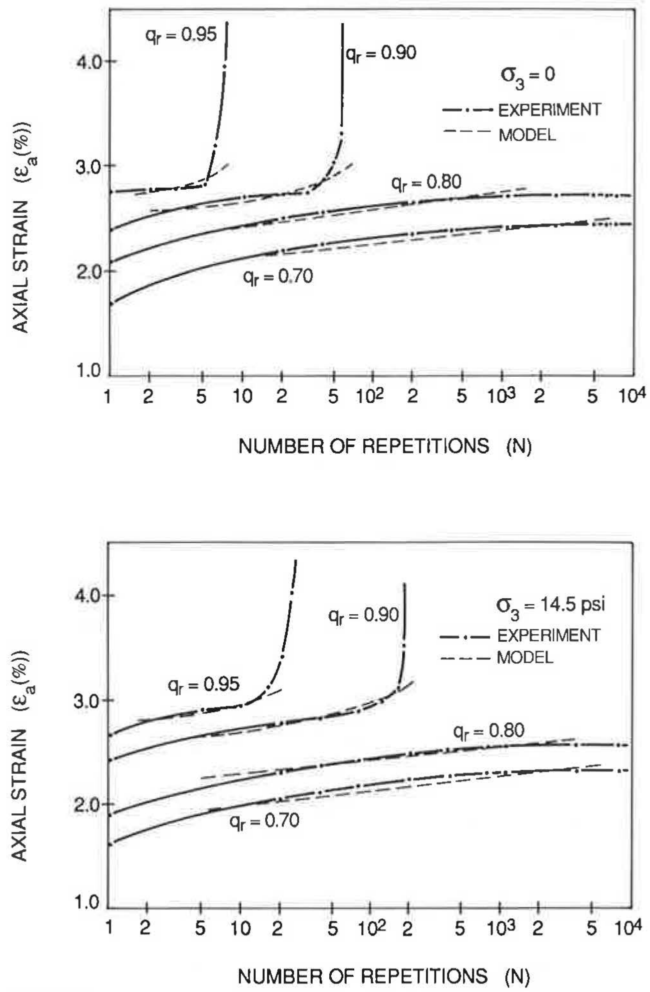

FIGURE 14 Verification of model predictions for specimens compacted dry of optimum (γ_d = 129.5 lb/ft^3, m = 7 percent).

TABLE 5 PARAMETERS USED IN THE PROPOSED SUBGRADE REPEATED-LOAD MODEL

		Subgrade repeated-load model: Low Stresses ($q_r \leq 0.80$) a_L	s_L	High Stresses ($q_r > 0.80$) a_h	B_h	S_h	Failure Strain ϵ_f (%)
Dry of optimum compaction	γ_d = 129.5 lb/cu ft, m = 7 %, σ_3 = 0	2.78	0.231	1.96	0.322	0.0586	2.82
	γ_d = 129.5 lb/cu ft, m = 7 %, σ_3 = 14.5 psi	2.74	0.160	1.85	0.371	0.0588	2.91
Wet of optimum compaction	γ_d = 129.5 lb/cu ft, m = 10 %, σ_3 = 0	5.25	0.648	4.30	0.0253	0.170	6.00
	γ_d = 129.5 lb/cu ft, m = 10 %, σ_3 = 14.5 psi	5.71	0.950	3.90	0.380	0.163	9.02

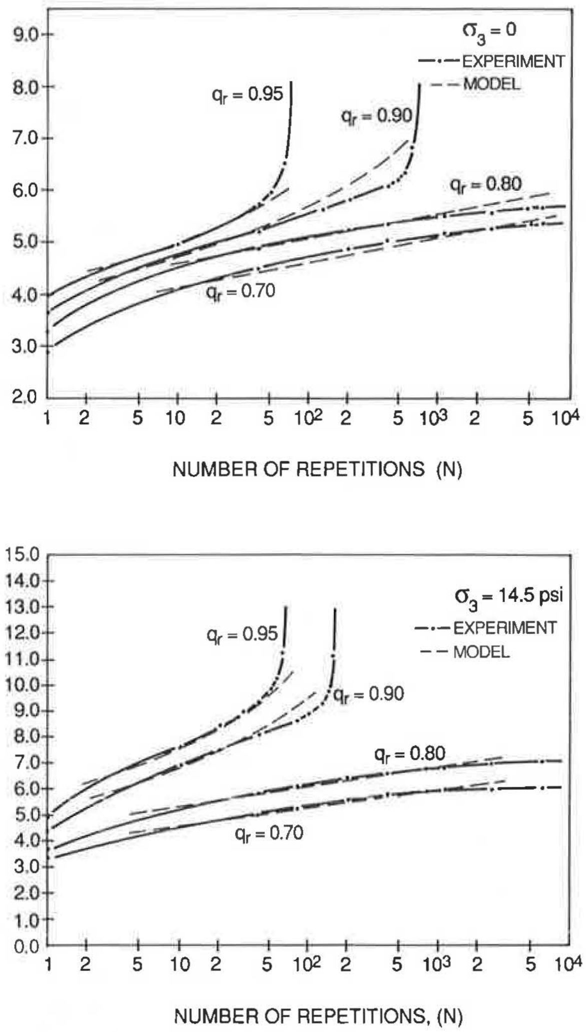

FIGURE 15 Verification of model predictions for specimens compacted wet of optimum (γ_d = 129.5 lb/ft^3, m = 10 percent).

REFERENCES

1. S. F. Brown and J. W. Pappin. Analysis of Pavements with Granular Basis. In *Transportation Research Record 810*, TRB, National Research Council, Washington, D.C., 1981, pp. 17–23.
2. L. Raad and J. L. Figueroa. Load Response of Transportation Support Systems. *Journal of the Transportation Engineering Division*, ASCE, Vol. 106, No. TE1, 1980, pp. 111–128.
3. C. L. Monismith, H. B. Seed, F. G. Mitry, and C. K. Chan. Prediction of Pavement Deflections from Laboratory Repeated Load Tests. *Proc., Second International Conference on the Structural Design of Asphalt Pavements*, 1968, pp. 109–410.
4. *Shell Pavement Design Manual: Asphalt Pavements and Overlays for Road Traffic.* Shell International Petroleum Company Limited, London, England, 1978.
5. M. I. Darter and A. J. Devos. *Structural Analysis of Asphaltic Cold Mixtures Used in Pavement Bases.* Project IHR-505, Research Report 505-4. University of Illinois, Engineering Experiment Station, Aug. 1977.
6. Y. T. Chou, R. L. Hutchinson, and H. H. Ulery, Jr. A Design Method for Flexible Airfield Pavements. In *Transportation Research Record 521*, TRB, National Research Council, Washington, D.C., 1974.
7. M. W. Witczak. Design of Full Depth Asphalt Airfield Pavements. *Proc., Third International Conference on the Structural Design of Asphalt Pavements*, London, England, 1972, pp. 550–567.
8. J. Poulsen and R. N. Stubstad. *Laboratory Testing of Intact Cohesive Subgrades: Results and Implications Relative to Structural Pavement Design and Distress Models.* Interim Report 76. National Danish Road Laboratory, November 1977.
9. W. A. Barker and W. N. Brabston. *Development of a Structural Design Procedure for Flexible Airport Pavements.* Technical Report S-75-17, Soils and Pavements Laboratory, U.S. Army Corps of Engineers Waterways Experiment Station, Vicksburg, Miss., Sept. 1975.
10. K. R. Peattie. A Fundamental Approach to the Design of Flexible Pavements. *Proc., International Conference on the Structural Design of Asphalt Pavements*, Ann Arbor, Mich., 1962, pp. 403–411.
11. R. D. Barksdale. *Repeated Load Testing Evaluation of Base Course Materials.* GHD Research Project 7002, Final Report. FHWA, U.S. Department of Transportation, 1972.
12. R. M. Knutson, M. R. Thompson, T. Mullin, and S. D. Tayabji. *Materials Evaluation Study.* Report FRA-OR and D-77-02. Ballast and Foundation Research Program, Federal Railroad Administration, Washington, D.C., 1977.
13. C. L. Monismith, K. Inkabi, C. R. Freeme, and D. B. McLean. A Subsystem to Predict Rutting in Asphalt Concrete Pavement Structures. *Proc., Fourth International Conference on the Structural Design of Asphalt Pavement*, Ann Arbor, Mich., 1977, pp. 529–539.
14. L. Raad, D. Weichert, and A. Haidar. Shakedown and Fatigue of Pavements with Granular Bases. In *Transportation Research Record 1227*, TRB, National Research Council, Washington, D.C., 1989.
15. Y. P. Vaid and R. G. Campanella. Time-Dependent Behavior of Undisturbed Clay. *Journal of the Geotechnical Engineering Division*, ASCE, Vol. 123, 1977, pp. 693–709.
16. J. K. Mitchell. *Fundamentals of Soil Behavior.* John Wiley and Sons, Inc., New York, 1976.
17. A. Ansal and A. Erken. Undrained Behavior of Clay Under Cyclic Shear Stress. *Journal of Geotechnical Engineering*, ASCE, Vol. 115, No. 7, 1989, pp. 968–983.
18. B. A. Zeid. *Load-Deformation Behavior of a Compacted Silty Clay Under Different Forms of Loading.* M.E. thesis. American University of Beirut, Beirut, Lebanon, 1988.
19. J. G. Larew and G. A. Leonards. A Strength Criterion for Repeated Loads. In *Highway Research Record 41*, HRB, National Research Council, Washington, D.C., 1962, pp. 529–556.
20. S. F. Brown, A. F. K. Lashine, and A. F. L. Hyde. Repeated Load Triaxial Testing of Silty Clay. *Geotechnique*, Vol. 25, No. 1, 1975, pp. 95–114.

Publication of this paper sponsored by Committee on Soil and Rock Properties.